



Published in final edited form as:

Cancer Res. 2020 March 01; 80(5): 964–975. doi:10.1158/0008-5472.CAN-19-1532.

## HIF-2-induced long non-coding RNA RAB11B-AS1 promotes hypoxia-mediated angiogenesis and breast cancer metastasis

Yanling Niu<sup>1</sup>, Lei Bao<sup>1</sup>, Yan Chen<sup>1</sup>, Chenliang Wang<sup>1</sup>, Maowu Luo<sup>1</sup>, Bo Zhang<sup>1</sup>, Mi Zhou<sup>1</sup>, Jennifer E. Wang<sup>1</sup>, Yisheng V. Fang<sup>1</sup>, Ashwani Kumar<sup>2</sup>, Chao Xing<sup>2,3,4</sup>, Yingfei Wang<sup>1,5,\*</sup>, Weibo Luo<sup>1,6,\*</sup>

<sup>1</sup>Department of Pathology, UT Southwestern Medical Center, Dallas, TX 75390, USA

<sup>2</sup>Eugene McDermott Center for Human Growth and Development, UT Southwestern Medical Center, Dallas, TX 75390, USA

<sup>3</sup>Department of Bioinformatics, UT Southwestern Medical Center, Dallas, TX 75390, USA

<sup>4</sup>Department of Population and Data Sciences, UT Southwestern Medical Center, Dallas, TX 75390, USA

<sup>5</sup>Department of Neurology and Neurotherapeutics, UT Southwestern Medical Center, Dallas, TX 75390, USA

<sup>6</sup>Department of Pharmacology, UT Southwestern Medical Center, Dallas, TX 75390, USA

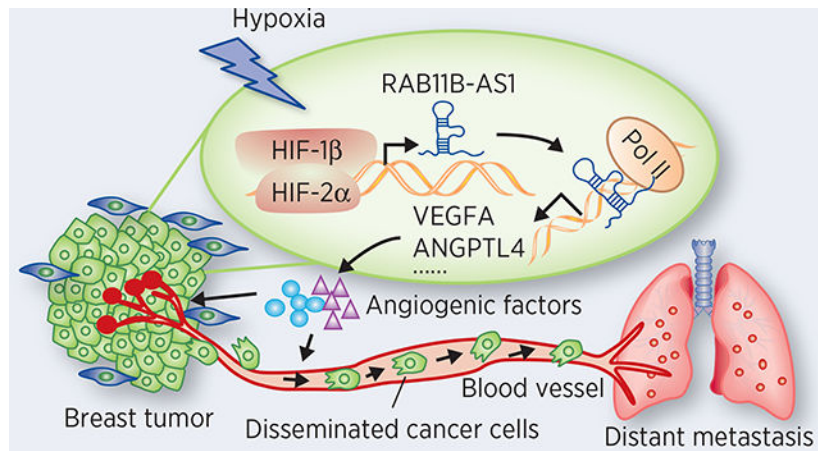
### Abstract

Hypoxia induces a vast array of long non-coding RNAs (lncRNAs) in breast cancer cells, but their biological functions remain largely unknown. Here we identified a hitherto uncharacterized hypoxia-induced lncRNA RAB11B-AS1 in breast cancer cells. RAB11B-AS1 is a natural lncRNA upregulated in human breast cancer and its expression is induced by hypoxia-inducible factor 2 (HIF-2), but not HIF-1, in response to hypoxia. RAB11B-AS1 enhanced the expression of angiogenic factors including VEGFA and ANGPTL4 in hypoxic breast cancer cells by increasing recruitment of RNA polymerase II. In line with increased angiogenic factors, conditioned media from RAB11B-AS1-overexpressing breast cancer cells promoted tube formation of human umbilical vein endothelial cells *in vitro*. Gain- and loss-of-function studies revealed that RAB11B-AS1 increased breast cancer cell migration and invasion *in vitro* and promoted tumor angiogenesis and breast cancer distant metastasis without affecting primary tumor growth in mice. Taken together, these findings uncover a fundamental mechanism of hypoxia-induced tumor angiogenesis and breast cancer metastasis.

### Graphical Abstract

\*Address correspondence to: Weibo Luo, Department of Pathology, UT Southwestern Medical Center, 5323 Harry Hines Blvd., NB6.460, Dallas, TX 75390-9072, USA. Phone: 214.645.4770; Weibo.Luo@UTSouthwestern.edu, Yingfei Wang, Department of Pathology, UT Southwestern Medical Center, 5323 Harry Hines Blvd., NB6.456, Dallas, TX 75390-9072, USA. Phone: 214.645.7691; Yingfei.Wang@UTSouthwestern.edu.

The authors declare no potential conflicts of interest.



HIF-2 induces expression of lncRNA RAB11B-AS1, which in turn increases the expression of angiogenic factors to promote angiogenesis and breast cancer metastasis.

### Keywords

Hypoxia; HIF; lncRNA; Angiogenesis; Metastasis; Breast cancer

### Introduction

Metastasis is responsible for about 90% of deaths due to breast cancer and targeting breast cancer metastasis remains a challenge. Long non-coding RNAs (lncRNAs) are a group of RNA transcripts longer than 200 nucleotides and have gained increasing attention because of their emerging role in gene regulation, which contributes to a wide range of cellular functions, including development, differentiation, cell fate, and disease pathogenesis (1–4). About 15,000 lncRNA transcripts have been identified in human genome by the GENCODE consortium in the ENCODE project (5). Several lncRNAs have been shown to play a critical role in breast cancer metastasis. For example, HOTAIR is highly expressed in metastatic breast cancer and promotes breast cancer metastasis by regulating polycomb repressive complex 2-dependent gene expression (6). TreRNA promotes breast cancer metastasis by suppressing the translation of E-Cadherin mRNA (7). LincRNA-ROR antagonizes miR-145 to activate the small GTPase ADP-ribosylation factor 6, which downregulates E-cadherin and disrupts cell-cell junctions, leading to invasion of triple-negative breast cancer cells (8). BCAR4 activates the chemokine CCL21-induced Hedgehog pathway and breast cancer metastasis by regulating the SNIP1-PNUTS-p300-RNA polymerase (Pol) II axis (9). Given a critical role of lncRNAs in metastatic breast cancer, it is of great importance to discover new lncRNAs and their role in the pathological processes of breast cancer metastasis.

Hypoxia is a hallmark of the microenvironment in breast tumors and promotes tumor progression and metastasis (10). The transcription factor hypoxia-inducible factor (HIF) is a key regulator of response to hypoxic stress in metazoans (11). HIF is a heterodimer of an oxygen-regulated  $\alpha$  subunit and a stably expressed  $\beta$  subunit (12). In mammals, the  $\alpha$  subunit is encoded by three distinct genes: *HIF1A*, *EPAS1*, and *HIF3A* (12–14), whereas the

$\beta$  subunit is encoded by *ARNT* and *ARNT2* genes (12,15). Under normoxia, HIF- $\alpha$  protein is hydroxylated on the proline residues by prolyl hydroxylase 2 and then rapidly degraded at the 26S proteasome by the ubiquitin E3 ligase von Hippel-Lindau/Cullin-2/Elongin-B/C (16). Upon hypoxia, HIF- $\alpha$  protein is stabilized and translocated into the nucleus, where it dimerizes with HIF- $\beta$ , allowing the heterodimer to bind the hypoxia response element (HRE) and then to activate the transcription of the downstream target genes (17). Extensive studies have discovered hundreds of HIF-induced protein-coding genes in cancer cells, whose protein products regulate the important cancer biology, including cancer cell stemness, autophagy, angiogenesis, metabolism, immune evasion, and metastasis (11). Although a recent genome-wide transcriptome study showed that hypoxia induces a vast array of lncRNAs in breast cancer MCF-7 cells (18), little is known about the function of hypoxia-induced lncRNAs in breast cancer.

In the present study, we reported that the lncRNA RAB11B-AS1 is transcriptionally induced by hypoxia in breast cancer cells in a HIF-2-dependent manner. RAB11B-AS1 enhances hypoxia-induced VEGFA and ANGPTL4 expression in breast cancer cells through RNA Pol II and promotes angiogenesis and distant breast cancer metastasis in mice. These findings uncover a novel mechanism of hypoxia-induced angiogenesis and breast cancer metastasis.

## Materials and Methods

### Cell culture, transfection, and virus

The culture conditions of MDA-MB-231 (from Rolf Brekken at UT Southwestern in 2015), MDA-MB-468 (from ATCC in 2017), SUM159, MCF-7, T47D, BT474, ZR-75-1, HCC1954, HeLa, HEK293FT, and HEK293T (from Gregg L. Semenza at Johns Hopkins in 2014) cells were described previously (19). Cells within six passages were used for experiments. Human umbilical vein endothelial cells (HUVECs) were cultured in M200PRF medium with low serum growth supplement (Thermo Fisher Scientific) at 37°C in a 5% CO<sub>2</sub>/95% air incubator. HUVECs within the first three passages were used for experiments. Hypoxic cells were placed in a modular incubator chamber (Billups-Rothenberg) and flushed with a gas mixture of 1% O<sub>2</sub>, 5% CO<sub>2</sub>, and balanced N<sub>2</sub>. Cells were transfected using PolyJet (SigmaGen). Lentiviruses encoding scrambled control (SC) or RAB11B-AS1 short hairpin RNAs (shRNAs) were generated as described previously (19). All cell lines except for HUVECs were annually tested to be mycoplasma-free and have been authenticated by STR DNA profiling analysis in 2016–2017.

### RNA extraction, RT-qPCR, and RNA-sequencing (RNA-seq) assays

Total RNA was isolated from the tissues or cultured cells using Trizol (Thermo Fisher Scientific), treated with DNase I (Thermo Fisher Scientific) and then subject to cDNA synthesis with the iScript cDNA synthesis kit (Bio-Rad). Quantitative real-time polymerase chain reaction (qPCR) was performed with iTaq universal SYBR green supermix (Bio-Rad) and normalized to the internal control 18S RNA or RPL13A as described previously (19). The primers used for qPCR are listed in Supplementary Table S1. RNA-seq was performed as described previously (19). The deidentified human breast tumors and benign breast tissues were used and their pathology was verified by a breast cancer pathologist (Y.V.F). The study

was approved by the Institutional Review Board at UT Southwestern Medical Center with informed written consent.

### 5' and 3' rapid amplification of cDNA ends (RACEs) assay

5'- and 3'-RACE analyses were performed using the SMARTer RACE 5'/3' kit (Takara Bio). Total RNA was extracted using the RNeasy micro kit (Qiagen) and treated with DNase. RNA integrity was assessed with the Agilent 4200 TapeStation system. After reverse transcription of total RNA to cDNA, 5'- and 3'-RACE PCRs were performed with the universal and gene-specific primers listed in Supplementary Table S2 and the resulting PCR products were cloned into linearized pRACE vector and sequenced. The nucleotide sequence of RAB11B-AS1 was deposited in the GenBank ([MK855053](#)).

### Plasmid constructs

Full-length human RAB11B-AS1 cDNA was cloned into pcDNA3.1 or pBluescript II KS (+). RAB11B-AS1 shRNA nucleotides (Supplementary Table S2) were cloned into pLKO.1 vector. HIF-1 $\beta$  single gRNA (sgRNA) nucleotides (Supplementary Table S2) were cloned into lentiCRISPRv2 vector. Wild-type (WT) or mutant *RAB11B-AS1* HRE nucleotides (Supplementary Table S2) were cloned into MluI/BglII-linearized pGL2p vector (Promega). All plasmids were verified by DNA sanger sequencing. Other plasmid constructs have been described previously (19).

### Luciferase reporter assay

$5 \times 10^4$  of HEK293T or HeLa cells were seeded onto 48-well plates pre-coated with poly-L-lysine a day prior to transfection. Cells were cotransfected with pGL2p-WT RAB11B-AS1 HRE, pGL2p-mutant RAB11B-AS1 HRE, or pGL2p-VEGFA HRE; pSV40-Renilla; and p3XFLAG-HIF-2 $\alpha$ , pcDNA3.1-RAB11B-AS1, or empty vector (EV) and exposed to 20% or 1% O<sub>2</sub> for 24 hours. Firefly and *Renilla* luciferase activities were measured using the Dual Luciferase Reporter Assay System (Promega).

### Immunoblot assay

Cells were lysed with NETN lysis buffer (150 mM NaCl, 1 mM EDTA, 50 mM Tris-HCl, pH8.0, 0.5% NP-40, and fresh protease inhibitor) and protein samples were separated by sodium dodecyl sulfate-polyacrylamide gel electrophoresis (SDS-PAGE), transferred to nitrocellulose membrane, and visualized by chemiluminescence with ECL prime (GE Healthcare) as described previously (19). The following antibodies were used: anti-HIF-1 $\alpha$  (BD Bioscience, Cat.# 610959), anti-HIF-2 $\alpha$  (Bethyl Laboratories, Cat.# A700-003), anti-HIF-1 $\beta$  (Novus Biologicals, Cat.# 100-110), RNA polymerase II (Abcam, Cat.# ab817), and anti- $\beta$ -actin (Proteintech, Cat.# 66009-1-Ig).

### Chromatin immunoprecipitation (ChIP) assay

Cells were cross-linked with 1% formaldehyde for 10 minutes, quenched in 0.125 M glycine, and lysed with lysis buffer followed by sonication. Then the lysates were incubated overnight at 4°C with anti-RNA Pol II antibody (Abcam, Cat.# ab817), anti-HIF-2 $\alpha$  antibody (homemade), anti-HIF-1 $\beta$  (Novus Biologicals, Cat.# 100-110), or IgG (Cell

Signaling Technology, Cat.# 2729S). After decrosslinking of the protein-DNA complex and DNA purification, precipitated DNA was subject to library preparation for sequencing or qPCR with primers listed in Supplementary Table S1. Bioinformatics analysis of ChIP-sequencing (ChIP-seq) data was performed as described previously (19). The RNA-seq and ChIP-seq data were deposited at the GEO database (GSE139861).

### RNA pulldown assay

The biotin-labeled sense and antisense of RAB11B-AS1 RNA were synthesized *in vitro* by T7 RNA polymerase (Thermo Fisher Scientific) using pBluescript-RAB11B-AS1 as a template and the biotin RNA labeling mix (Sigma). The RNAs were denatured, refolded in RNA structure buffer (10 mM Tris-HCl, pH 7.0, 0.1 M KCl, and 10 mM MgCl<sub>2</sub>), and incubated for 2 hours at 4 °C in the presence of 0.1 µg/µL tRNA, 0.025% BSA, and the pre-cleared lysates, which were extracted from MDA-MB-231 cells exposed to 20% or 1% O<sub>2</sub> for 24 hours in RNA immunoprecipitation buffer (150 mM KCl, 25 mM Tris-HCl, pH7.4, 5 mM EDTA, 0.5% NP-40, 0.5 mM DTT, fresh protease inhibitor, and RNase inhibitor). 0.25% BSA-prebound streptavidin magnetic beads (GE Healthcare) were added for additional 1-hour incubation at 4 °C. The proteins bound to biotin-labeled RAB11B-AS1 RNA were separated by SDS-PAGE and analyzed by immunoblot assay.

### Boyden chamber migration and invasion assays

Cell migration and invasion assays were performed as described previously (19).  $2 \times 10^4$  of cells were suspended in serum-free media and seeded onto the non-coated (migration) or Matrigel-coated (invasion) upper chamber. 10% FBS in the bottom chamber was used as a chemoattractant. Cells were exposed to 20% or 1% O<sub>2</sub> for 16 hours (migration) or 24 hours (invasion), fixed with methanol, and stained with 0.1% crystal violet. Colonies were imaged using microscope and counted in five randomly selected fields at 20x magnification.

### *In vitro* angiogenesis assay

$4 \times 10^4$  of HUVECs were starved in M200PRF medium without low serum growth supplement for 2 hours, resuspended in fresh conditional media with 1% FBS, and seeded onto a 96-well plate coated with growth factor-reduced Matrigel (BD Biosciences). Conditional media were collected by incubating MDA-MB-231-EV or -RAB11B-AS1 cells with serum-free DMEM for 24 hours. HUVECs were imaged using the IncuCyte S3 live-cell analysis system (Sartorius) for 5 hours and the total tube length from five randomly selected fields at 10x magnification was measured by the Wimasis image analysis.

### Animal studies

Six-eight weeks old female NOD/SCID IL2R $\gamma$ null (NSG) mice were used for animal studies, which has been approved and conducted under the oversight of the UT Southwestern Institutional Animal Care and Use Committee. For the orthotopic xenograft model,  $2 \times 10^6$  of breast cancer cells suspended in PBS/Matrigel (1:1, Corning) were implanted into the second left mammary fat pad of female NSG mice. Tumor growth was monitored with a caliper every 3 days starting 14 days after implantation and calculated with the formula: volume = 0.52  $\times$  length  $\times$  height  $\times$  width. Mice were euthanized 32–40 days

after cell implantation and primary tumors were harvested. After perfusion with PBS, the whole lungs were inflated with low-melt agarose and analyzed by haematoxylin and eosin (H&E) staining. The whole liver was also collected for H&E staining. Genomic DNA was extracted from the whole lungs and liver and analyzed by qPCR assay with primers for human *HK2* gene and mouse and human 18S rRNA. For the tail vein injection model,  $1 \times 10^6$  of breast cancer cells suspended in 100  $\mu$ L PBS were injected into the tail vein of female NSG mice. Three weeks later, the lungs were harvested for H&E staining and qPCR analysis with primers for human *HK2* gene and mouse and human 18S rRNA. The area of metastatic foci was quantified by ImageJ and normalized to the total area of lung or liver tissues.

### Immunohistochemistry (IHC) assay

IHC assay was performed by the Dako Autostainer Link 48 system (Dako) as described (19). The tissue slides underwent deparaffinication, rehydration, and epitope retrieval and were then incubated with the primary antibody: Endomucin (Santa Cruz Biotechnology, 1:50), Cleaved caspase-3 (CC3, Cell Signaling Technology, 1:1500), and Ki-67 (Proteintech, 1:1000). Staining was visualized using the EnVision FLEX visualization system (Dako). The endomucin-, Ki-67-, and CC3-positive areas were quantified by ImageJ and normalized to their respective total area.

### Statistical analysis

Statistical analysis was performed by Student's *t* test with or without Welch's correction between two groups, and one-way or two-way ANOVA with multiple testing correction within multiple groups. RNA-seq and ChIP-seq were performed in duplicate and other experiments were repeated at least three times. Data were expressed as mean  $\pm$  SEM.  $p < 0.05$  is considered significant.

## Results

### RAB11B-AS1 is induced by hypoxia in breast cancer cells in a HIF-2-dependent manner

Our RNA-seq studies (GSE108833) showed that RAB11B-AS1 was a hypoxia-inducible lncRNA in human breast cancer MDA-MB-231 cells. To validate, we performed RT-qPCR in a panel of human breast cancer cell lines, including MDA-MB-231, MDA-MB-468, SUM159, MCF-7, T47D, BT474, ZR-75-1, and HCC1954, exposed to 20% or 1% O<sub>2</sub> for 24 hours. RAB11B-AS1 RNA levels were significantly upregulated by hypoxia in all breast cancer cell lines we tested (Fig. 1A). RAB11B-AS1 is an antisense RNA of the *RAB11B* gene. To annotate the natural transcript of RAB11B-AS1 in breast cancer cells, we performed 5'- and 3'-RACE and detected a specific 1037-nucleotide RAB11B-AS1 transcript in MDA-MB-231 cells (Fig. 1B; Supplementary Fig. S1). The RAB11B-AS1 transcript had 10 more A nucleotides in the poly(A) tail at its 3' end but missed 7 nucleotides at the 5' end as compared with the reference transcript deposited in the GenBank (NR\_038237.1, Supplementary Fig. S1). In addition, there were two nucleotide mutations in the exons 2&3 (Supplementary Fig. S1). Together, these data indicate that RAB11B-AS1 is a natural lncRNA and induced by hypoxia in breast cancer cells.

To determine whether HIF is required for hypoxia-induced RAB11B-AS1 in breast cancer cells, we performed RT-qPCR assay in parental, HIF-1 $\alpha$  knockout (KO), HIF-2 $\alpha$  KO, HIF-1 $\alpha$  and HIF-2 $\alpha$  double knockout (DKO) MDA-MB-231 cells exposed to 20% or 1% O<sub>2</sub> for 24 hours. HIF-2 $\alpha$  KO, but not HIF-1 $\alpha$  KO, eliminated hypoxia-induced RAB11B-AS1 expression in MDA-MB-231 cells (Fig. 1C). Similar results were also found in HIF-1 $\alpha$  and HIF-2 $\alpha$  DKO cells under hypoxia (Fig. 1C). KO of HIF-1 $\alpha$  or HIF-2 $\alpha$  in MDA-MB-231 cells were confirmed by determining the expression of HIF-1 $\alpha$  and HIF-2 $\alpha$  (Fig. 1D). Likewise, KO of HIF-1 $\beta$  abolished hypoxia-induced RAB11B-AS1 expression in MDA-MB-231 cells (Fig. 1E and F). These data indicate that HIF-2 is responsible for hypoxia-induced RAB11B-AS1 expression in breast cancer cells.

To unbiasedly identify the HRE on the *RAB11B-AS1* gene, we performed ChIP-seq assay in hypoxic MDA-MB-231 cells and found a robust HIF-2 $\alpha$  peak annotated with the HRE sequence 5'-ACGTG-3' at the promoter of the *RAB11B-AS1* gene (Fig. 2A). To validate, we performed ChIP-qPCR in MDA-MB-231 cells exposed to 20% or 1% O<sub>2</sub> for 24 hours. HIF-2 $\alpha$  was enriched at this HRE, but not on the non-target gene *RPL13A* (Fig. 2B and C). Hypoxia significantly increased HIF-2 $\alpha$  occupancy at the RAB11B-AS1 HRE (Fig. 2B). Similarly, HIF-1 $\beta$  occupancy was detected at the RAB11B-AS1 HRE in hypoxic MDA-MB-231 cells (Fig. 2D). To examine whether this HRE is functional, a 60-base pair DNA fragment containing the HRE was cloned into the upstream of the SV40 promoter and firefly luciferase gene in a pGL2p reporter vector. HEK293T cells were transfected with pGL2p-EV or pGL2p-RAB11B-AS1 HRE, and the control plasmid pSV40-Renilla, and exposed to 20% or 1% O<sub>2</sub> for 24 hours. The RAB11B-AS1 HRE significantly enhanced firefly luciferase activity in HEK293T cells under hypoxia as compared with the EV, but failed to do so in non-hypoxic cells (Fig. 2E), where no HIF-2 $\alpha$  protein is present due to its proteasomal degradation, indicating the specificity of the RAB11B-AS1 HRE in response to hypoxia. Mutation of 5'-CGT-3' into 5'-AAA-3' within the RAB11B-AS1 HRE completely abolished hypoxia-induced firefly luciferase activity in HEK293T cells (Fig. 2E). Moreover, ectopic expression of HIF-2 $\alpha$  significantly increased RAB11B-AS1 HRE-driven firefly luciferase activity in non-hypoxic and hypoxic HEK293T cells (Fig. 2F; Supplementary Fig. S2A). In contrast, HIF-2 $\alpha$  KO significantly inhibited hypoxia-induced RAB11B-AS1 HRE activity in HeLa cells (Fig. 2G; Supplementary Fig. S2B). Collectively, these data indicate that *RAB11B-AS1* is a direct HIF-2 target gene in human breast cancer cells.

### **RAB11B-AS1 increases breast cancer cell migration and invasion *in vitro***

To determine the oncogenic role of RAB11B-AS1 in breast cancer cells, we next generated RAB11B-AS1-overexpressed MDA-MB-231 cells. RT-qPCR assay showed about 14-fold increase in RAB11B-AS1 RNA levels in these cells (Fig. 3A). The Boyden transwell assay showed that ectopic expression of RAB11B-AS1 significantly increased migration and invasion of MDA-MB-231 cells under 20% and 1% O<sub>2</sub> as compared with the EV (Fig. 3B–E). Similar results were also observed in SUM159 cells (Supplementary Fig. S3A–E). These data indicate that RAB11B-AS1 overexpression promotes breast cancer cell migration/invasion *in vitro*.

To complement gain-of-function studies, we next performed loss-of-function studies by generating two independent RAB11B-AS1 knockdown (KD) MDA-MB-231 cell lines via lentiviral infection. About 80–90% of RAB11B-AS1 KD efficiency was achieved in either of cell lines under hypoxia (Fig. 3F). Hypoxia increased migration of SC MDA-MB-231 cells by more than 1.5-fold, whereas RAB11B-AS1 KD significantly inhibited cell migration under 20% and 1% O<sub>2</sub> (Fig. 3G and H). Similarly, the number of cells invaded through Matrigel was also significantly decreased by RAB11B-AS1 KD under 20% and 1% O<sub>2</sub> (Fig. 3I and J). Likewise, RAB11B-AS1 KD also significantly reduced migration and invasion of SUM159 or MDA-MB-468 cells under 20% and 1% O<sub>2</sub> (Supplementary Fig. S3F–O). Together, gain- and loss-of-function studies indicate that RAB11B-AS1 promotes breast cancer cell motility *in vitro*.

### **RAB11B-AS1 promotes tumor angiogenesis and breast tumor metastasis in mice**

To investigate the effect of RAB11B-AS1 on breast cancer cell motility *in vivo*, we implanted EV or RAB11B-AS1-overexpressed MDA-MB-231 cells orthotopically into the mammary fat pad of female NSG mice. Ectopic expression of RAB11B-AS1 in MDA-MB-231 cells did not affect primary tumor growth in mice (Fig. 4A–C). RT-qPCR assay confirmed > 20-fold increase in RAB11B-AS1 RNA levels in RAB11B-AS1 tumors (Fig. 4D). The blood vessel marker endomucin-positive area was significantly increased in RAB11B-AS1 tumors as compared to EV tumors (Fig. 4E and F), whereas the area percentage of staining of Ki-67, a marker for cell proliferation, was comparable in these tumors (Fig. 4E and G). RAB11B-AS1 did not alter the percentage of the cell death marker CC3-positive area in tumors (Supplementary Fig. S4A and B), suggesting that RAB11B-AS1 has no effect on caspase-3-dependent cell death in breast tumors. Notably, H&E analysis in the lungs revealed more spontaneous metastases in mice bearing RAB11B-AS1 tumors than EV tumors (Fig. 4H and I), which was confirmed by analysis of the presence of human genomic DNA in mouse lungs with qPCR (Fig. 4J). Similarly, ectopic expression of RAB11B-AS1 significantly increased MDA-MB-231 cell metastasis to the liver in mice (Fig. 4K–M).

Next, we performed loss-of-function studies in the orthotopic breast cancer mouse model. In line with gain-of-function studies above (Fig. 4A–C), RAB11B-AS1 KD in MDA-MB-231 cells did not affect primary tumor growth in NSG mice (Fig. 5A–C). RT-qPCR assay confirmed robust RAB11B-AS1 KD in tumors (Fig. 5D). IHC analysis showed the density of endomucin-positive blood vessels was significantly decreased in RAB11B-AS1 KD1 or KD2 tumors as compared to SC tumors (Fig. 5E and F). In contrast, Ki-67 staining was comparable between SC and RAB11B-AS1 KD tumors (Fig. 5E and G), in line with gain-of-function studies (Fig. 4E and G). Both H&E and qPCR assays showed decreased spontaneous breast cancer metastasis to the lungs and liver in mice bearing RAB11B-AS1 KD tumors as compared to those with SC tumors (Fig. 5H–M).

To investigate whether RAB11B-AS1 regulates breast cancer cell colonization to increase distant metastasis, we injected SC or RAB11B-AS1 KD1 or KD2 MDA-MB-231 cells into the tail vein of female NSG mice. The lungs were harvested three weeks later. H&E staining detected extensive tumor foci in the lungs from SC tumor bearing mice (Fig. 5N and O). In



contrast, fewer breast cancer cells were present in the lungs from mice bearing RAB11B-AS1 KD1 or KD2 tumors (Fig. 5N and O). qPCR assay further confirmed that RAB11B-AS1 KD significantly reduced breast cancer cell colonization in the lungs (Fig. 5P). Collectively, these findings indicate that RAB11B-AS1 increases tumor angiogenesis and promotes breast cancer metastasis to distant organs in mice without affecting primary tumor growth.

### **RAB11B-AS1 enhances hypoxia-induced angiogenic factors in breast cancer cells through the recruitment of RNA Pol II**

To dissect the molecular mechanism of RAB11B-AS1-induced tumor angiogenesis, we investigated whether RAB11B-AS1 regulates the expression of angiogenic factors in breast cancer cells. RNA-seq assay identified 1526 upregulated genes and 1677 downregulated genes in RAB11B-AS1-overexpressed MDA-MB-231 cells under hypoxia (FDR > 0.05, LogCPM > 0, fold change > 1.25, Fig. 6A). Gene ontology analysis of upregulated genes revealed that angiogenesis and response to hypoxia were two of top biological processes (Supplementary Table S3). To validate, we performed RT-qPCR assay in EV and RAB11B-AS1-overexpressed MDA-MB-231 cells exposed to 20% or 1% O<sub>2</sub> for 24 hours. Consistently, ectopic expression of RAB11B-AS1 significantly increased the VEGFA mRNA expression in non-hypoxic and hypoxic MDA-MB-231 cells (Fig. 6B). Interestingly, ANGPTL4 mRNA was also enhanced by RAB11B-AS1 overexpression in non-hypoxic and hypoxic MDA-MB-231 cells (Fig. 6B), despite not being selected as the RAB11B-AS1 target gene according to our selection criteria in RNA-seq (Fig. 6A). Similar results were also observed in SUM159 cells (Supplementary Fig. S5A). Complementary to gain-of-function studies, RAB11B-AS1 KD by either of two shRNAs significantly decreased hypoxia-induced VEGFA and ANGPTL4 mRNAs in MDA-MB-231 and MDA-MB-468 cells (Fig. 6C; Supplementary Fig. S5B). Reduction of VEGFA and ANGPTL4 mRNAs was very modest or little in RAB11B-AS1 KD MDA-MB-231 and MDA-MB-468 cells exposed to 20% O<sub>2</sub> (Fig. 6C; Supplementary Fig. S5B). Other angiogenic factors including ANGPT2, CXCR4, FN1, MMP9, and bFGF were not significantly affected by RAB11B-AS1 KD1 or KD2 (Supplementary Fig. S5C). Ectopic expression or KD of RAB11B-AS1 failed to affect the mRNA levels of RAB11B and RPL13A in MDA-MB-231, MDA-MB-468, or SUM159 cells (Fig. 6B and C; Supplementary Fig. S5). These data indicate that RAB11B-AS1 increases hypoxia-induced angiogenic factors including VEGFA and ANGPTL4 in breast cancer cells.

Next, we studied whether angiogenic factors induced by RAB11B-AS1 in breast cancer cells regulates angiogenesis *in vitro*. Conditional culture media from EV or RAB11B-AS1-overexpressed MDA-MB-231 cells were collected and incubated with HUVECs. After 5-hour incubation, the length of tubes was significantly increased in HUVECs cultured with RAB11B-AS1 conditional media as compared to EV conditional media (Fig. 6D and E). These data indicate that RAB11B-AS1 increases the expression of angiogenic factors in breast cancer cells to promote angiogenesis *in vitro*, which supports our *in vivo* findings (Fig. 4E and F).

RNA Pol II binding to the gene promoter is an essential step in transcriptional regulation. Gene ontology of RAB11B-AS1-upregulated genes identified RNA Pol II-dependent gene regulation as the top biological function, implicating that RNA Pol II may be involved in RAB11B-AS1-mediated gene regulation (Supplementary Table S3). To determine the role of RNA Pol II in RAB11B-AS1-mediated VEGFA and ANGPTL4 expression, we studied whether RAB11B-AS1 interacts with RNA Pol II by RNA pull-down assay. *In vitro* transcribed biotin-labeled RAB11B-AS1 RNA was incubated in the presence of streptavidin magnetic beads with lysates of MDA-MB-231 cells exposed to 20% or 1% O<sub>2</sub> for 24 hours. Endogenous RNA Pol II was strongly pulled down by RAB11B-AS1 RNA, but barely bound to beads only (Fig. 6F). We further studied whether RAB11B-AS1 regulates RNA Pol II binding to VEGFA and ANGPTL4 genes by RNA Pol II ChIP-qPCR assay. RNA Pol II was enriched at the promoter of VEGFA and ANGPTL4 genes and its enrichment was significantly increased by hypoxia in MDA-MB-231 cells (Fig. 6G and H). RAB11B-AS1 KD significantly reduced RNA Pol II occupancy at the promoter of VEGFA and ANGPTL4 genes in hypoxic MDA-MB-231 cells (Fig. 6G and H), which was consistent with their reduced gene expression in RAB11B-AS1 KD cells under hypoxia (Fig. 6C; Supplementary Fig. S5). RAB11B-AS1 KD had no effect on RNA Pol II binding to the RPL13A gene in MDA-MB-231 cells (Fig. 6I). These findings indicate that RAB11B-AS1 promotes RNA Pol II binding to VEGFA and ANGPTL4 genes under hypoxia to increase their expression in breast cancer cells.

It has been known that HIF induces VEGFA and ANGPTL4 in cancer cells to promote tumor angiogenesis and metastasis (19). We studied the role of HIF in RAB11B-AS1-mediated VEGFA and ANGPTL4 expression. RNA pull-down assay showed that HIF-1 $\alpha$  and HIF-2 $\alpha$  both failed to bind to sense or anti-sense of RAB11B-AS1 RNA (Supplementary Fig. S6A). The stability of HIF-1 $\alpha$  and HIF-2 $\alpha$  proteins is critical for HIF transcriptional activity (16). Ectopic expression or KD of RAB11B-AS1 did not affect HIF-1 $\alpha$  and HIF-2 $\alpha$  protein levels in MDA-MB-231 cells (Supplementary Fig. S6B and C). We further performed HIF luciferase reporter assay to determine whether RAB11B-AS1 regulates HIF transcriptional activity. HEK293T cells were cotransfected with a HIF reporter plasmid, which contains 2  $\times$  VEGFA HRE upstream of the SV40 promoter and firefly luciferase coding gene, and pSV40-Renilla, and RAB11B-AS1 expression vector or EV, and exposed to 20% or 1% O<sub>2</sub> for 24 hours. Ectopic expression of RAB11B-AS1 had no effect on HIF transcriptional activity in non-hypoxic and hypoxic HEK293T cells (Supplementary Fig. S6D). Together, these data indicate that HIF is not directly involved in RAB11B-AS1-mediated VEGFA and ANGPTL4 expression in hypoxic breast cancer cells.

### **RAB11B-AS1 RNA is upregulated in human breast tumors**

To study clinical relevance of RAB11B-AS1, we analyzed its expression in human breast tumors and control benign breast tissues. RAB11B-AS1 RNA levels were significantly higher in human breast tumors as compared to control breast tissues (Fig. 7A). Likewise, VEGFA and ANGPTL4 mRNAs were also upregulated in human breast tumors (Fig. 7B and C). The Pearson correlation analysis revealed that RAB11B-AS1 RNA expression was significantly correlated with VEGFA or ANGPTL4 mRNA expression in human breast

tumors (Fig. 7D and E). These data indicate that RAB11B-AS1 RNA is upregulated and correlated with VEGFA and ANGPTL4 mRNAs in human breast tumors.

## Discussion

Since thousands of lncRNAs have been identified in human genome by genome-wide gene analysis, it becomes clear that the expression of lncRNAs is differentially regulated by various stimuli in the tissue- and cell type-specific manners. In the present study, we for the first time annotated the nucleotide sequence of human RAB11B-AS1 in MDA-MB-231 cells by 5' and 3' RACE assays and showed that RAB11B-AS1 is a hypoxia-inducible lncRNA in breast cancer cells. Hypoxia induction of RAB11B-AS1 occurs in all subtypes of human breast cancer cell lines, indicating that hypoxia is a general mechanism of regulation of RAB11B-AS1 expression in breast cancer. Our CHIP, luciferase reporter, and RT-qPCR data revealed that HIF-2, but not HIF-1, controls RAB11B-AS1 transcription in hypoxic breast cancer cells. Previous studies showed that hypoxia upregulates a subset of lncRNAs in MCF-7 cells (18), and several lncRNAs, including NEAT1, MALAT1, and UCA1, have been characterized to be regulated by HIF-1 and/or HIF-2 in breast cancer cells (20–22). As lncRNAs display tissue-specific expression patterns (5), further studies are needed to determine whether RAB11B-AS1 is also induced by HIF-2 in normal and malignant cells from other tissues besides breast.

Accumulating evidence reveals that lncRNA plays an important role in gene regulation and several mechanistic models have been proposed (23). Our gain- and loss-of-function studies showed that RAB11B-AS1 enhances the expression of angiogenic factors including VEGFA and ANGPTL4 in breast cancer cells exposed to hypoxia. The expression of the *RAB11B* gene is not regulated by RAB11B-AS1 in breast cancer cells, although both genes are partially overlapped as shown by our RACE data. *ANGPTL4* also locates next to the *RAB11B-AS1* gene in the genome, but *VEGFA* locates on the different chromosome 6, suggesting that a *trans*-regulatory mechanism may contribute to RAB11B-AS1-mediated VEGFA and ANGPTL4 expression. Indeed, RAB11B-AS1 interacts with RNA Pol II and controls RNA Pol II binding to the promoter of *VEGFA* and *ANGPTL4* genes to enhance their expression in hypoxic MDA-MB-231 cells. Although *VEGFA* and *ANGPTL4* are both known HIF target genes (19), RAB11B-AS1 fails to increase HIF transcriptional activity, and thus it is unlikely that HIF is directly involved in RAB11B-AS1-mediated VEGFA and ANGPTL4 expression under hypoxia. Collectively, our findings reveal that the RAB11B-AS1-RNA Pol II axis represents a previously unrecognized mechanism of hypoxia-induced expression of angiogenic factors in breast cancer (Fig. 7F).

Similar to protein-coding genes, lncRNAs participate in multiple cellular signaling pathways, including oncogenic signaling (24). Our present studies showed that RAB11B-AS1 increases the expression of a subset of angiogenic factors including VEGFA and ANGPTL4 in hypoxic breast cancer cells. In line with regulation of these angiogenic factors, RAB11B-AS1 promotes angiogenesis *in vitro* and in xenograft tumors. Angiogenesis promotes breast cancer metastasis to distant organs (25), suggesting that RAB11B-AS1-mediated angiogenesis may contribute to breast cancer metastasis at least in the xenograft mouse model that mimics spontaneous metastasis. Further studies are needed to investigate

its role in the clinical model of metastasis and if additional mechanisms are also involved in RAB11B-AS1-mediated breast cancer metastasis as RAB11B-AS1 controls dysregulation of many genes in breast cancer cells under hypoxia. Notably, primary breast tumor growth is not affected by RAB11B-AS1 overexpression or KD. In accordance with this, RAB11B-AS1 fails to regulate the expression of the cell proliferation marker Ki-67 in xenograft tumors. These findings reveal that RAB11B-AS1 is a metastasis-associated lncRNA in breast cancer. A previous study reported that RAB11B-AS1 abrogates osteosarcoma cell proliferation, migration, and invasion *in vitro* and suppresses osteosarcoma growth *in vivo* (26). Thus, RAB11B-AS1 may function as both oncogene and tumor suppressor in a tissue-specific manner. The tissue-specific functions have been similarly observed for other lncRNAs, such as H19 (27,28).

In summary, we identified a novel HIF-2 target lncRNA RAB11B-AS1 in breast cancer cells. RAB11B-AS1 is induced by hypoxia and in turn increases the expression of angiogenic factors including VEGFA and ANGPTL4 in hypoxic breast cancer cells through the recruitment of RNA Pol II, leading to tumor angiogenesis and metastasis (Fig. 7F). These findings provide novel mechanistic insights into breast cancer progression and uncover RAB11B-AS1 as a possible target for the treatment of metastatic breast cancer.

## Supplementary Material

Refer to Web version on PubMed Central for supplementary material.

## Acknowledgments

We thank Ondine Cleaver (UT Southwestern) for HUVECs and the UTSW Cancer Center Tissue Resource for assistance in immunohistochemistry. This work was supported by grants from the Susan G. Komen® (CCR16376227), the NIH (R01CA222393, R00CA168746), the CPRIT (RR140036, RP190358), and the Welch Foundation (I-1903) to W.L., and the NIH (R00NS078049, R35GM124693, and R01AG066166), the CPRIT (RP170671), and the Welch Foundation (I-1939) to Y.W.. W.L. is a CPRIT Scholar in Cancer Research.

**Financial support:** Y.N. (CPRIT); L.B. (NIH, Welch); Y.C. (Susan G Komen); C.W. (CPRIT); M.L. (Susan G Komen); B.Z. (CPRIT); M. Z. (CPRIT); J.E.W. (NIH); Y.V.F. (UTSW); A. K. (UTSW); C. X. (UTSW); Y.W. (NIH, CPRIT, Welch, UTSW); W.L. (NIH, CPRIT, Welch, Susan G Komen, UTSW)

## References

1. Serviss JT, Johnsson P, Grander D. An emerging role for long non-coding RNAs in cancer metastasis. *Front Genet* 2014;5:234 [PubMed: 25101115]
2. Fatica A, Bozzoni I. Long non-coding RNAs: new players in cell differentiation and development. *Nat Rev Genet* 2014;15:7–21 [PubMed: 24296535]
3. Flynn RA, Chang HY. Long noncoding RNAs in cell-fate programming and reprogramming. *Cell Stem Cell* 2014;14:752–61 [PubMed: 24905165]
4. Kazemzadeh M, Safaralizadeh R, Orang AV. LncRNAs: emerging players in gene regulation and disease pathogenesis. *J Genet* 2015;94:771–84 [PubMed: 26690535]
5. Derrien T, Johnson R, Bussotti G, Tanzer A, Djebali S, Tilgner H, et al. The GENCODE v7 catalog of human long noncoding RNAs: analysis of their gene structure, evolution, and expression. *Genome Res* 2012;22:1775–89 [PubMed: 22955988]
6. Gupta RA, Shah N, Wang KC, Kim J, Horlings HM, Wong DJ, et al. Long non-coding RNA HOTAIR reprograms chromatin state to promote cancer metastasis. *Nature* 2010;464:1071–6 [PubMed: 20393566]

7. Gumireddy K, Li A, Yan J, Setoyama T, Johannes GJ, Orom UA, et al. Identification of a long non-coding RNA-associated RNP complex regulating metastasis at the translational step. *EMBO J* 2013;32:2672–84 [PubMed: 23974796]
8. Eades G, Wolfson B, Zhang Y, Li Q, Yao Y, Zhou Q. lincRNA-RoR and miR-145 regulate invasion in triple-negative breast cancer via targeting ARF6. *Mol Cancer Res* 2015;13:330–8 [PubMed: 25253741]
9. Xing Z, Lin A, Li C, Liang K, Wang S, Liu Y, et al. lncRNA directs cooperative epigenetic regulation downstream of chemokine signals. *Cell* 2014;159:1110–25 [PubMed: 25416949]
10. Luo W, Wang Y. Hypoxia Mediates Tumor Malignancy and Therapy Resistance. *Adv Exp Med Biol* 2019;1136:1–18 [PubMed: 31201713]
11. Semenza GL. Hypoxia-inducible factors: mediators of cancer progression and targets for cancer therapy. *Trends Pharmacol Sci* 2012;33:207–14 [PubMed: 22398146]
12. Wang GL, Jiang BH, Rue EA, Semenza GL. Hypoxia-inducible factor 1 is a basic-helix-loop-helix-PAS heterodimer regulated by cellular O<sub>2</sub> tension. *Proc Natl Acad Sci U S A* 1995;92:5510–4 [PubMed: 7539918]
13. Tian H, McKnight SL, Russell DW. Endothelial PAS domain protein 1 (EPAS1), a transcription factor selectively expressed in endothelial cells. *Genes Dev* 1997;11:72–82 [PubMed: 9000051]
14. Gu YZ, Moran SM, Hogenesch JB, Wartman L, Bradfield CA. Molecular characterization and chromosomal localization of a third alpha-class hypoxia inducible factor subunit, HIF3alpha. *Gene Expr* 1998;7:205–13 [PubMed: 9840812]
15. Hirose K, Morita M, Ema M, Mimura J, Hamada H, Fujii H, et al. cDNA cloning and tissue-specific expression of a novel basic helix-loop-helix/PAS factor (Arnt2) with close sequence similarity to the aryl hydrocarbon receptor nuclear translocator (Arnt). *Mol Cell Biol* 1996;16:1706–13 [PubMed: 8657146]
16. Kaelin WG Jr., Ratcliffe PJ. Oxygen sensing by metazoans: the central role of the HIF hydroxylase pathway. *Mol Cell* 2008;30:393–402 [PubMed: 18498744]
17. Luo W, Wang Y. Epigenetic regulators: multifunctional proteins modulating hypoxia-inducible factor-alpha protein stability and activity. *Cell Mol Life Sci* 2018;75:1043–56 [PubMed: 29032501]
18. Choudhry H, Schodel J, Oikonomopoulos S, Camps C, Grampp S, Harris AL, et al. Extensive regulation of the non-coding transcriptome by hypoxia: role of HIF in releasing paused RNAPol2. *EMBO Rep* 2014;15:70–6 [PubMed: 24363272]
19. Chen Y, Zhang B, Bao L, Jin L, Yang M, Peng Y, et al. ZMYND8 acetylation mediates HIF-dependent breast cancer progression and metastasis. *J Clin Invest* 2018;128:1937–55 [PubMed: 29629903]
20. Choudhry H, Albukhari A, Morotti M, Haider S, Moralli D, Smythies J, et al. Tumor hypoxia induces nuclear paraspeckle formation through HIF-2alpha dependent transcriptional activation of NEAT1 leading to cancer cell survival. *Oncogene* 2015;34:4546 [PubMed: 26289678]
21. Lelli A, Nolan KA, Santambrogio S, Goncalves AF, Schonenberger MJ, Guinot A, et al. Induction of long noncoding RNA MALAT1 in hypoxic mice. *Hypoxia (Auckl)* 2015;3:45–52 [PubMed: 27774481]
22. Xue M, Li X, Li Z, Chen W. Urothelial carcinoma associated 1 is a hypoxia-inducible factor-1alpha-targeted long noncoding RNA that enhances hypoxic bladder cancer cell proliferation, migration, and invasion. *Tumour Biol* 2014;35:6901–12 [PubMed: 24737584]
23. Long Y, Wang X, Youmans DT, Cech TR. How do lncRNAs regulate transcription? *Sci Adv* 2017;3:eaao2110 [PubMed: 28959731]
24. Evans JR, Feng FY, Chinnaiyan AM. The bright side of dark matter: lncRNAs in cancer. *J Clin Invest* 2016;126:2775–82 [PubMed: 27479746]
25. Bielenberg DR, Zetter BR. The Contribution of Angiogenesis to the Process of Metastasis. *Cancer J* 2015;21:267–73 [PubMed: 26222078]
26. Chen Z, Liu Z, Yang Y, Zhu Z, Liang R, Huang B, et al. Long non-coding RNA RAB11B-AS1 prevents osteosarcoma development and progression via its natural antisense transcript RAB11B. *Oncotarget* 2018;9:26770 [PubMed: 29928484]

27. Lottin S, Adriaenssens E, Dupressoir T, Berteaux N, Montpellier C, Coll J, et al. Overexpression of an ectopic H19 gene enhances the tumorigenic properties of breast cancer cells. *Carcinogenesis* 2002;23:1885–95 [PubMed: 12419837]
28. Hao Y, Crenshaw T, Moulton T, Newcomb E, Tycko B. Tumour-suppressor activity of H19 RNA. *Nature* 1993;365:764–7 [PubMed: 7692308]

Author Manuscript

Author Manuscript

Author Manuscript

Author Manuscript

**Significance**

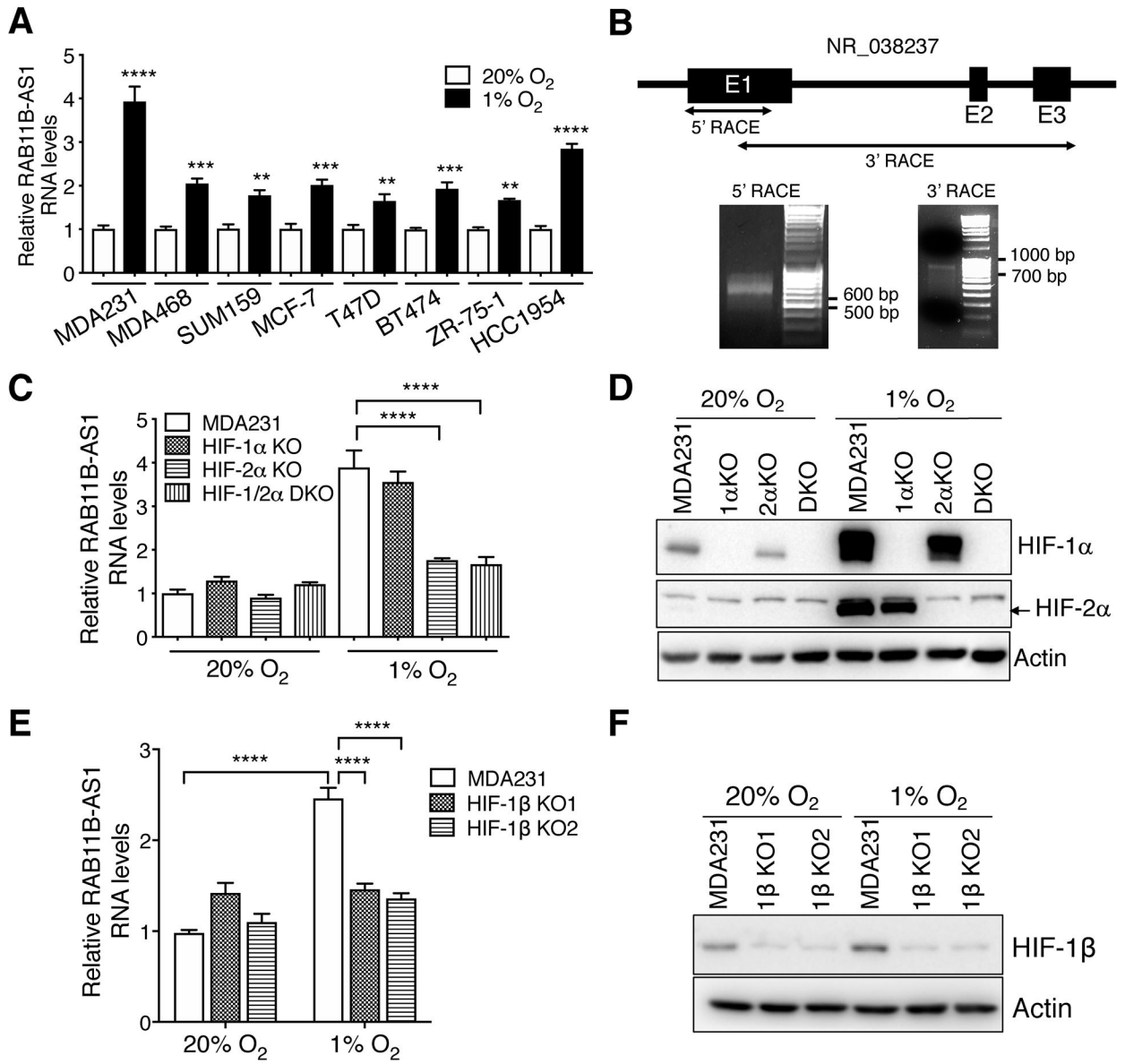
This study reveals the molecular mechanism by which the lncRNA RAB11B-AS1 regulates hypoxia-induced angiogenesis and breast cancer metastasis, and provides new insights into the functional interaction between a lncRNA and tumor microenvironment.

Author Manuscript

Author Manuscript

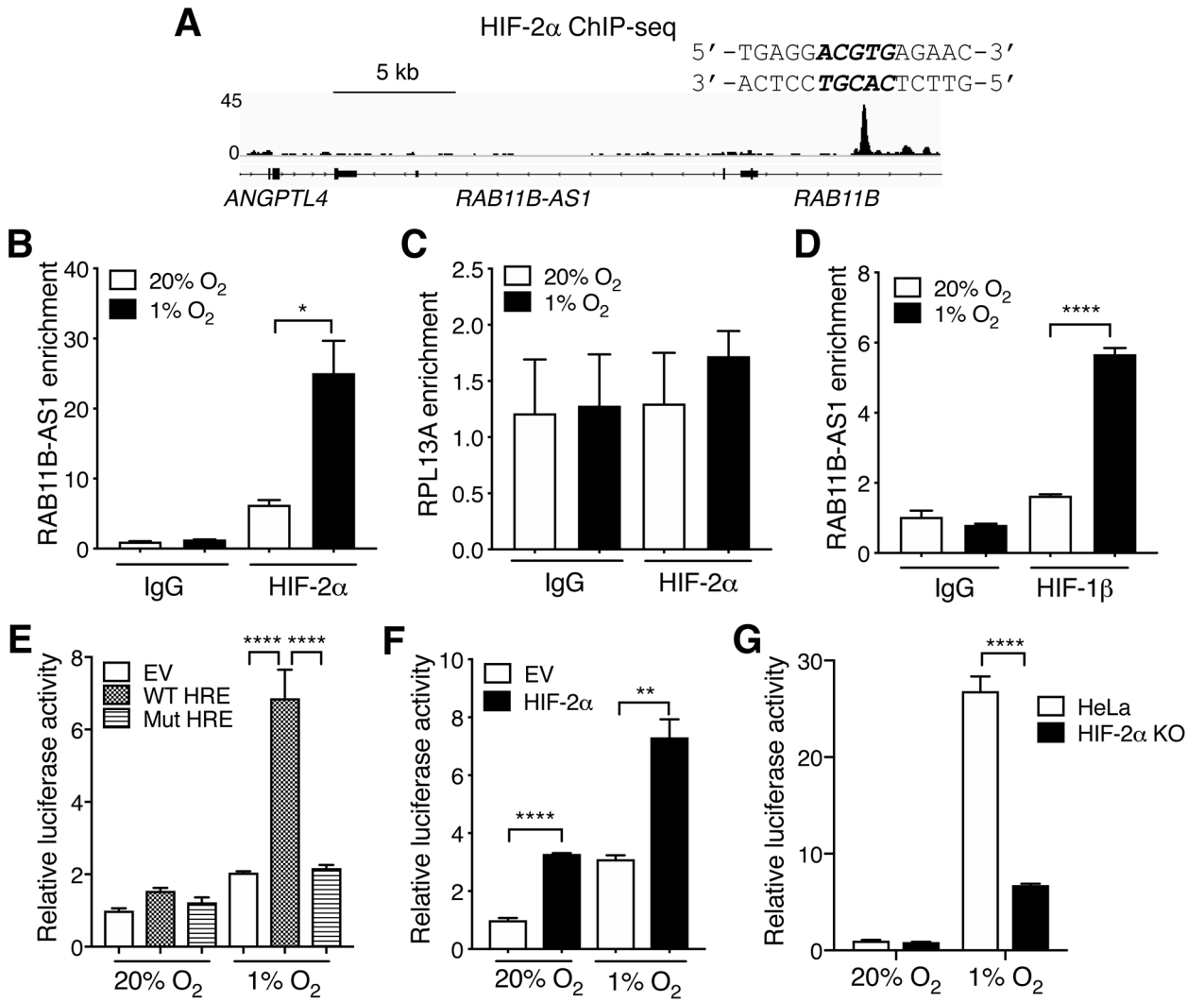
Author Manuscript

Author Manuscript

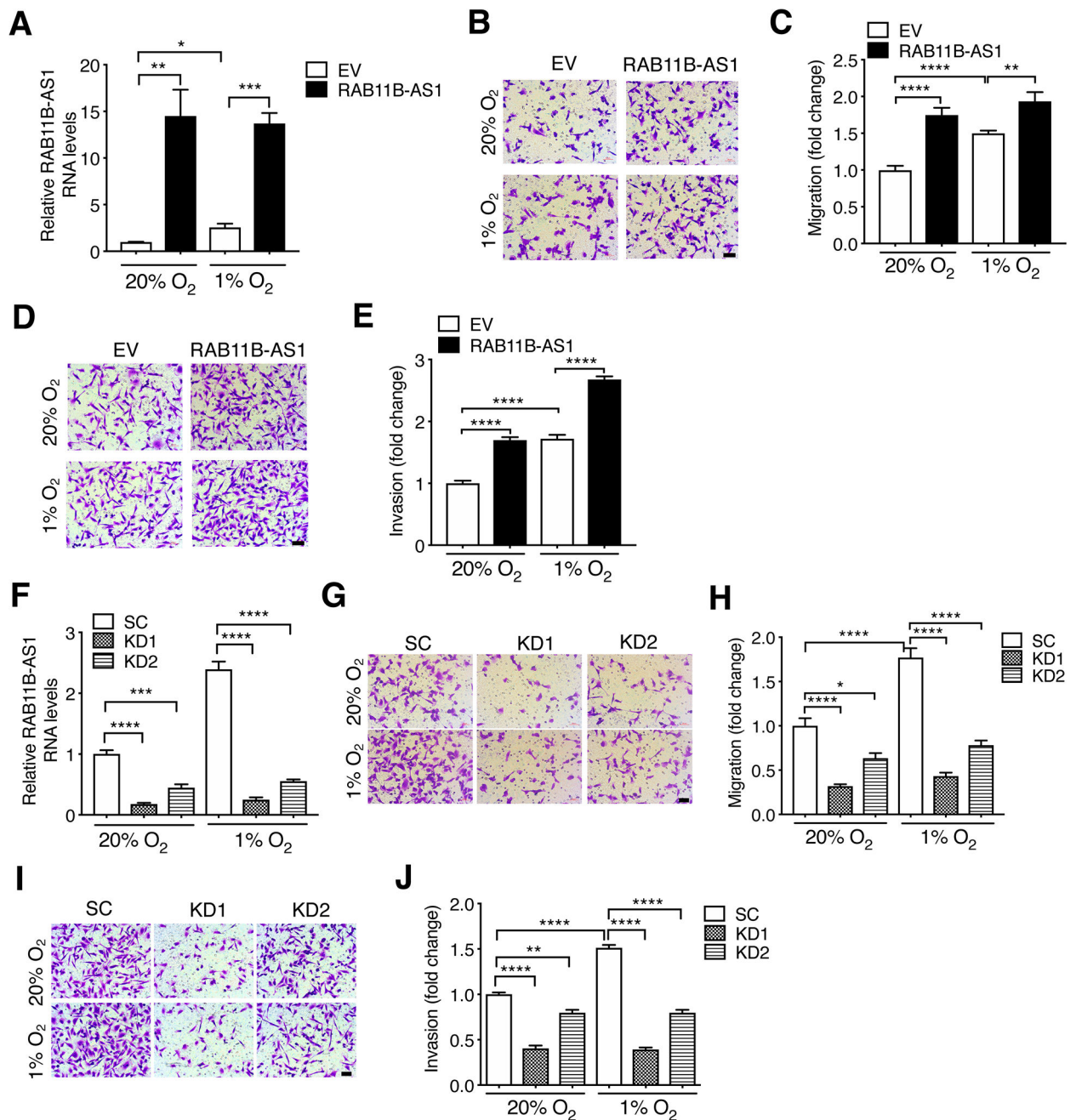


**Figure 1.** RAB11B-AS1 is induced by hypoxia in breast cancer cells in a HIF-2-dependent manner. **A**, RAB11B-AS1 RNA levels in breast cancer cell lines exposed to 20% or 1% O<sub>2</sub> for 24 hours. MDA231, MDA-MB-231; MDA468, MDA-MB-468. **B**, 5' and 3' RACE amplicons of RAB11B-AS1 using total RNA isolated from MDA-MB-231 exposed to 1% O<sub>2</sub> for 24 hours as a template. The location of 5' and 3' RACE PCR amplicons at the *RAB11B-AS1* gene is illustrated on the top. bp, base pair. E, exon. **C-F**, RAB11B-AS1 RNA levels and HIF protein levels in parental, HIF-1α KO (**C**, **D**), HIF-2α KO (**C**, **D**), HIF-1/2α DKO (**C**, **D**), and HIF-1β KO (**E**, **F**) MDA-MB-231 cells exposed to 20% or 1% O<sub>2</sub> for 24 hours (mean ± SEM, *n* = 3). \*\**p* < 0.01, \*\*\**p* < 0.001, \*\*\*\**p* < 0.0001.

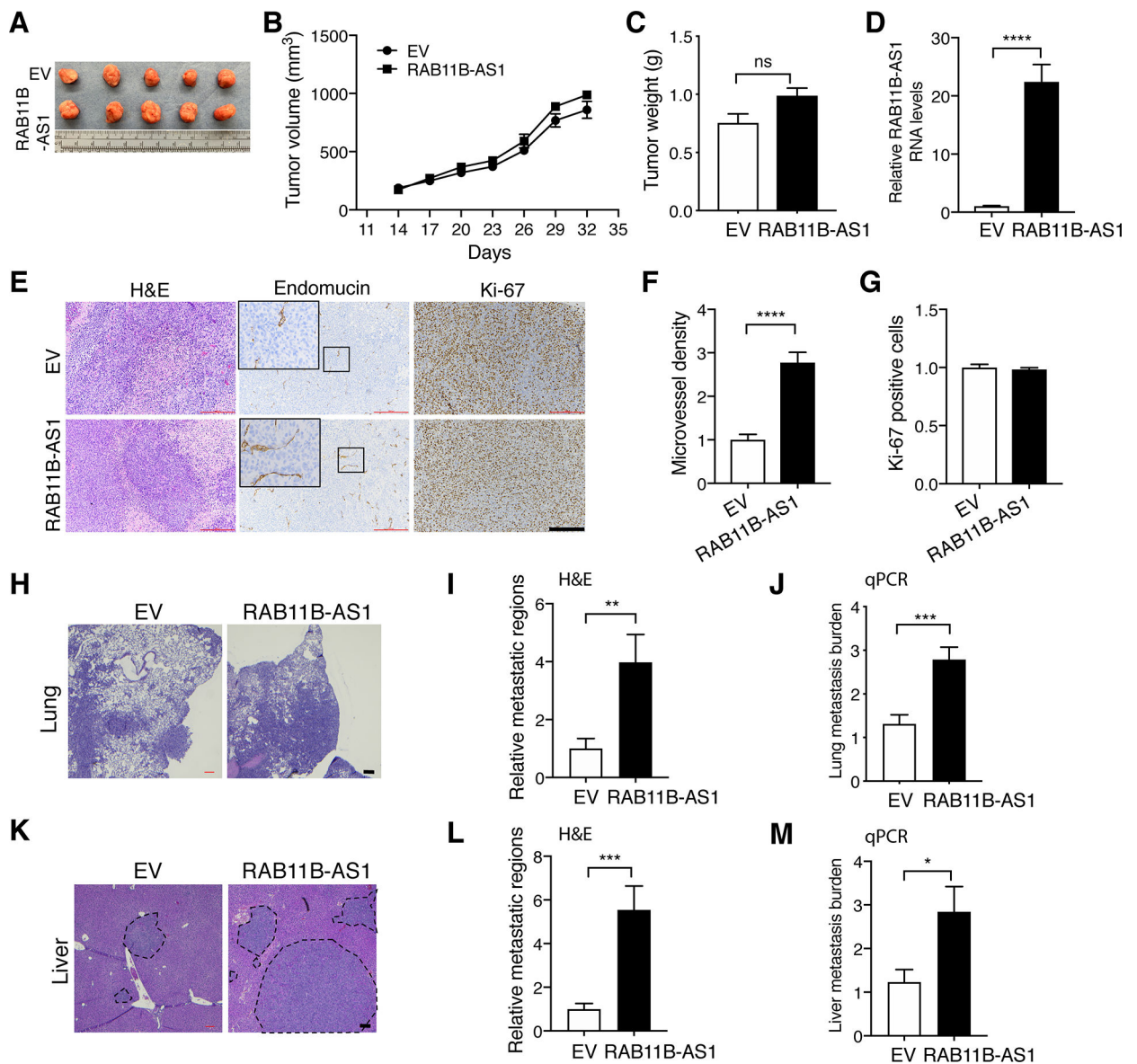




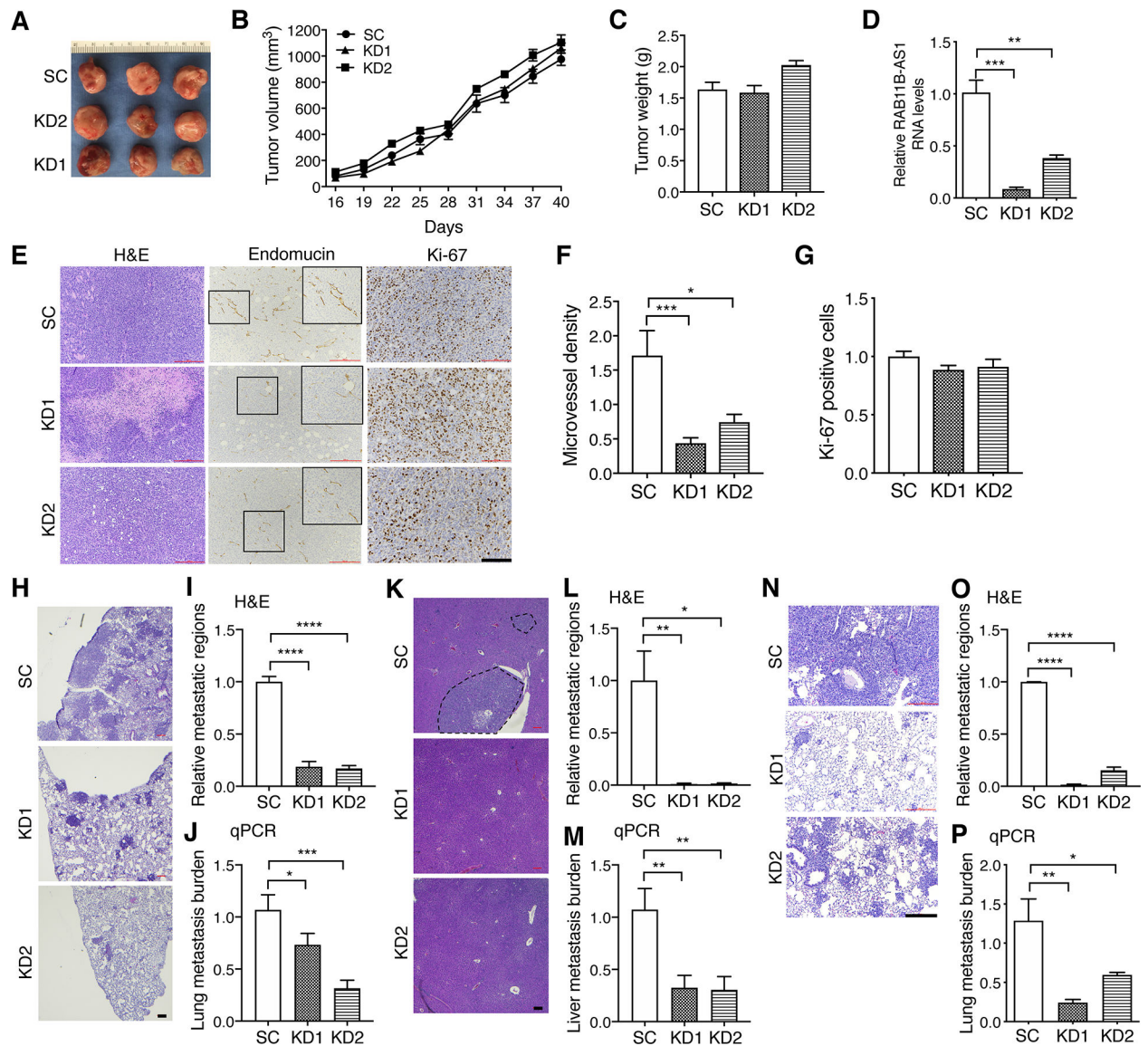
**Figure 2.** *RAB11B-AS1* is a direct HIF-2 target gene. **A**, The genome browser snapshot of HIF-2α ChIP peak at the *RAB11B-AS1* locus. The putative RAB11B-AS1 HRE (bold and italic) is shown. **B-D**, ChIP-qPCR analysis of HIF-2α (**B**, **C**) and HIF-1β (**D**) enrichment at the RAB11B-AS1 HRE or RPL13A in MDA-MB-231 cells exposed to 20% or 1% O<sub>2</sub> for 24 hours. **E-G**, RAB11B-AS1 HRE luciferase reporter assay in HEK293T (**E**, **F**) and HeLa cells (**G**) exposed to 20% or 1% O<sub>2</sub> for 24 hours. Firefly/*Renilla* luciferase activities were normalized to EV or parental at 20% O<sub>2</sub> (mean ± SEM, *n* = 3–4). \**p* < 0.05, \*\**p* < 0.01, \*\*\*\**p* < 0.0001. Mut, mutant.



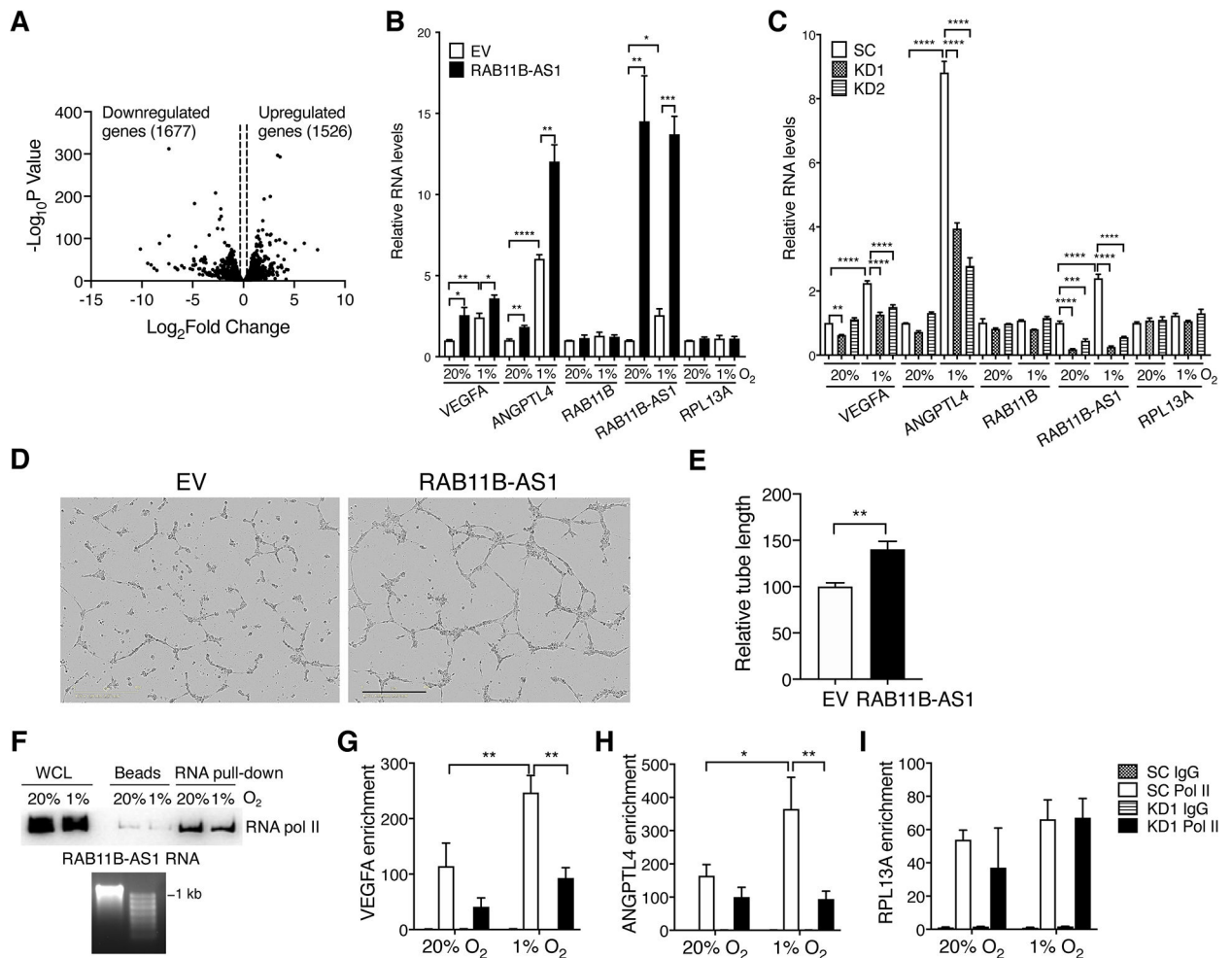
**Figure 3.** RAB11B-AS1 increases breast cancer cell migration and invasion *in vitro*. **A**, Overexpression of RAB11B-AS1 in MDA-MB-231 cells exposed to 20% or 1% O<sub>2</sub> for 24 hours. **B-D**, Effect of RAB11B-AS1 overexpression on cell migration (**B, C**) and invasion (**D, E**) under 20% and 1% O<sub>2</sub>. **F**, KD of RAB11B-AS1 in MDA-MB-231 cells exposed to 20% or 1% O<sub>2</sub> for 24 hours. **G-J**, Effect of RAB11B-AS1 KD on cell migration (**G, H**) and invasion (**I, J**) under 20% and 1% O<sub>2</sub>. Data are expressed as mean ± SEM,  $n = 3$ . \* $p < 0.05$ , \*\* $p < 0.01$ , \*\*\* $p < 0.001$ , \*\*\*\* $p < 0.0001$ . Scale bar, 50  $\mu\text{m}$ .



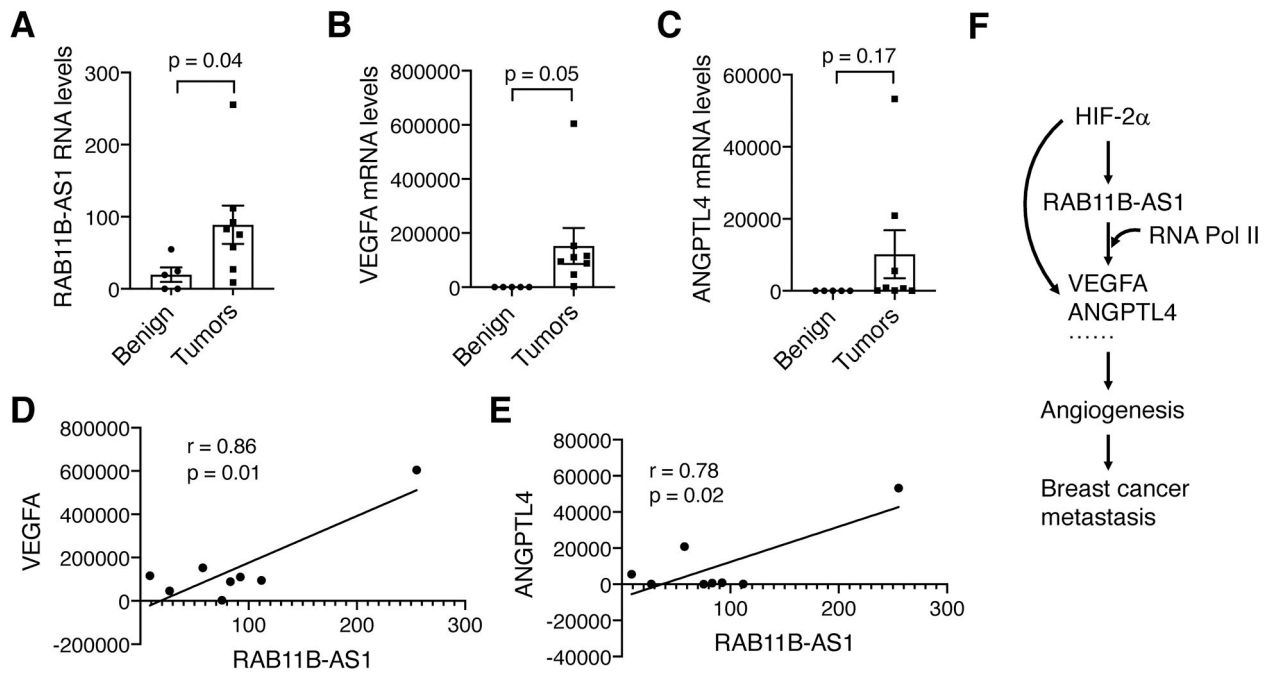
**Figure 4.** RAB11B-AS1 overexpression promotes tumor angiogenesis and breast cancer metastasis in mice. **A-D**, Effect of RAB11B-AS1 overexpression on breast tumor growth in NSG mice. The tumor image (**A**), growth curve (**B**), weight (**C**), and RAB11B-AS1 levels in tumors (**D**) are shown (mean  $\pm$  SEM,  $n = 5$ ). ns, not significant. **E-G**, Representative H&E and IHC of endomucin and Ki-67 and their quantification in MDA-MB-231-EV or -RAB11B-AS1 tumors (mean  $\pm$  SEM,  $n = 5$ ). Scale bar, 1 mm. **H-M**, Representative H&E and qPCR analysis of lung (**H-J**) and liver (**K-M**) metastasis in mice bearing MDA-MB-231-EV or -RAB11B-AS1 tumors (mean  $\pm$  SEM,  $n = 8-15$ ). Scale bar, 200  $\mu$ m. \* $p < 0.05$ , \*\* $p < 0.01$ , \*\*\* $p < 0.001$ , \*\*\*\* $p < 0.0001$ .



**Figure 5.** RAB11B-AS1 KD inhibits breast cancer metastasis in mice. **A-D**, Effect of RAB11B-AS1 KD on breast tumor growth in NSG mice. The tumor image (**A**), growth curve (**B**), weight (**C**), and RAB11B-AS1 levels in tumors (**D**) are shown (mean  $\pm$  SEM,  $n = 3$ ). **E-G**, Representative H&E and IHC of endomucin and Ki-67 and their quantification in SC and RAB11B-AS1 KD MDA-MB-231 tumors (mean  $\pm$  SEM,  $n = 3$ ). Scale bar, 1 mm. **H-M**, Representative H&E and qPCR analysis of lung (**H-J**) and liver (**K-M**) metastasis in mice bearing SC and RAB11B-AS1 KD MDA-MB-231 tumors (mean  $\pm$  SEM,  $n = 6-9$ ). Scale bar, 200  $\mu$ m. **N-P**, Representative H&E and quantification of SC and RAB11B-AS1 KD MDA-MB-231 cell colonization in the lungs (mean  $\pm$  SEM,  $n = 3-5$ ). Scale bar, 1 mm. \* $p < 0.05$ , \*\* $p < 0.01$ , \*\*\* $p < 0.001$ , \*\*\*\* $p < 0.0001$ .

**Figure 6.**

RAB11B-AS1 increases hypoxia-induced VEGFA and ANGPTL4 expression in breast cancer cells through recruiting RNA Pol II. **A**, Volcano plot of RAB11B-AS1-regulated genes in MDA-MB-231 cells under hypoxia ( $n = 2$ ). **B** and **C**, RT-qPCR analysis of indicated RNAs in RAB11B-AS1 overexpressed (**B**) and KD (**C**) MDA-MB-231 cells exposed to 20% or 1%  $\text{O}_2$  for 24 hours (mean  $\pm$  SEM,  $n = 3$ ). **D** and **E**, *In vitro* angiogenesis of HUVECs incubated with conditional media from EV or RAB11B-AS1-overexpressed MDA-MB-231 cells (mean  $\pm$  SEM,  $n = 6$ ). **F**, RNA pull-down assay of biotin-labeled RAB11B-AS1 RNA and lysates from MDA-MB-231 cells exposed to 20% or 1%  $\text{O}_2$  for 24 hours. **G-I**, ChIP-qPCR analysis of RNA Pol II enrichment at the promoter of the *VEGFA*, *ANGPTL4*, and *RPL13A* in SC and RAB11B-AS KD1 MDA-MB-231 cells exposed to 20% or 1%  $\text{O}_2$  for 24 hours (mean  $\pm$  SEM,  $n = 3$ ). \* $p < 0.05$ , \*\* $p < 0.01$ , \*\*\* $p < 0.001$ , \*\*\*\* $p < 0.0001$ .

**Figure 7.**

RAB11B-AS1 is upregulated and correlated with VEGFA and ANGPTL4 in human breast tumors. **A-C**, RT-qPCR analysis of RAB11B-AS1 RNA (**A**), VEGFA mRNA (**B**), and ANGPTL4 mRNA (**C**) in human breast tumors and benign breast tissues (mean  $\pm$  SEM,  $n = 5-8$ ). **D** and **E**, Pearson correlation analysis between RAB11B-AS1 expression and VEGFA (**D**) or ANGPTL4 (**E**) expression in human breast tumors. **F**, A proposed model for RAB11B-AS1-mediated angiogenesis and breast tumor metastasis. RAB11B-AS1 is induced by HIF-2 in response to hypoxia and increases hypoxia-induced VEGFA and ANGPTL4 expression in breast cancer cells, leading to tumor angiogenesis and metastasis in mice.